PAPER

Paintable temperature-responsive cholesteric liquid crystal reflectors encapsulated on a single flexible polymer substrate

Hitesh Khandelwal, Ellen P. A. van Heeswijk, [ID] Albert P. H. J. Schenning [ID] and Michael G. Debije [ID] *

This work describes the fabrication of temperature-responsive light reflectors deposited on flexible single substrates, a photonic cholesteric liquid crystal system encapsulated by a protective polymer layer generated by photo-enforced stratification. A bendable orange reflector was fabricated by this single application step. Furthermore, a blue shift of 400 nm of an infrared cholesteric reflector was demonstrated upon increasing the temperature from room temperature to 100 °C. Such reflectors on flexible substrates could be used for the retrofitting of existing windows to save energy and visible reflectors in clothing or other aesthetically pleasing applications.

Introduction

The generation of responsive reflective elements is a topic of current research.[1–5] Of particular interest are reflectors that respond to changes in temperature.[6,7] Visible color shifts provide striking visual cues that can be employed in security features and healthcare, or as aesthetic features. However, reflective elements in the otherwise invisible infrared (IR) region of the spectra could have at least as great a commercial impact as visible reflectors.

Buildings account for around 40% of energy use in Europe,[8] and even more in other regions.[9] An increasing fraction of this energy is used in air conditioning,[10] to counter the heating of interior spaces generated from sunlight entering through windows.[11] Infrared (IR) absorbers and reflectors have been developed with the goal of gaining a degree of control over the influx of IR light.[12–15] A disadvantage of many absorbers is that they also affect visible light, requiring the use of artificial lighting as compensation, an undesirable result. Many of the reflectors are also static, and cannot respond to changing environmental conditions.

Previous work has described temperature-responsive photonic reflectors, many based on chiral nematic (cholesteric) liquid crystals (LCs).[16–23] Cholesteric LC systems are able to reflect light as a result of their self-organized molecular helices. Because of their liquid nature, these systems show a large temperature response but need to be sandwiched between two glass plates (in a cell architecture),[16,24–26] which may not be practical or feasible

Laboratory of Stimuli-Responsive Functional Materials & Devices, Department of Chemical Engineering and Chemistry, Eindhoven University of Technology, P. O. Box 513, 5600 MB, Eindhoven, The Netherlands. E-mail: m.g.debije@tue.nl

in some instances, and in many cases, the temperature response of these polymers is limited and/or requires adsorbents.[27] Therefore, it remains a challenge to prepare temperature-responsive photonic coatings that are easily processable and show a large response.

Penterman *et al.* developed a paint containing a mixture of reactive and non-reactive monomers, an ultraviolet-light-absorbing dye, and a photoinitiator that can be used to fabricate liquid crystal displays (LCDs) on a rigid glass substrate by using a photo enforced stratification process.[28] Inspired by this work, we report the fabrication of low molecular mass cholesteric LC coatings formed on flexible polymer substrates using similar methods. We describe a bendable orange cholesteric LC reflector in an encapsulated polymer layer and a temperature responsive cholesteric LC which undergoes a blue shift of 400 nm in the infrared region at elevated temperatures.

Experimental

Two primary cholesteric LC mixtures were used in this work. The visible light reflecting mixture consists of 46.8 wt% nematic LC MLC-6653 (Merck), 44.5 wt% isobornyl methacrylate (IBMA, Sigma Aldrich), 4 wt% Bisphenol A dimethacrylate (BPAMA, Sigma Aldrich), 4 wt% chiral dopant S1011 (Merck), 0.4 wt% photoinitiator Irgacure 819 (Ciba Chemicals) and 0.3 wt% UV absorber Tinuvin-328 (Ciba Chemicals). The second mixture used for the fabrication of temperature responsive IR reflectors on single substrates consists of 36.3 wt% MLC-6653, 43.7 wt% IBMA, 3.7 wt% BPAMA, 15.2 wt% of temperature responsive chiral dopant TCD (Philips Research Lab), 0.5 wt% Irgacure 819

This journal is © The Royal Society of Chemistry 2019

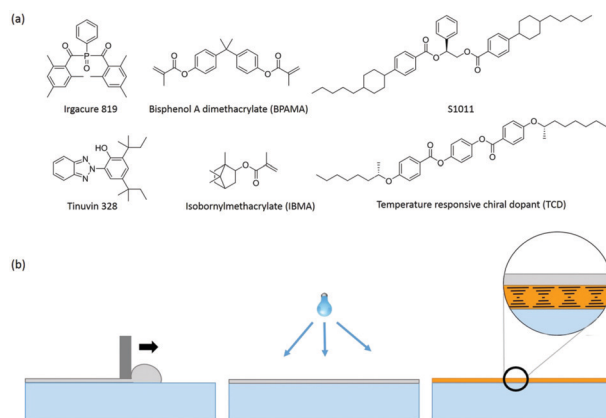*J. Mater. Chem. C*, 2019, **7**, 7395–7398 | 7395

Fig. 1 (a) Chemical structures of the materials used. (b) Diagram showing the mechanism used to fabricate the polymer encapsulating cholesteric LCs *via* bar coating followed by polymerization under UV light, and finally photo-enforced stratification of the polymer (gray) and cholesteric LC (orange) layers (based on the visual in ref. 28).

and 0.6 wt% Tinuvin 328. The chemical structures of all materials are shown in Fig. 1a.

The mixtures are bar coated directly on flexible 500 μm 8040T polycarbonate substrates (Sabic IP). The substrate was then placed in a nitrogen environment at 45 °C and illuminated with a 365 nm LED lamp (Thorlabs) for 20 min at ∼0.8 mW cm⁻² to promote stratification. The samples were then exposed to high-intensity UV for a few minutes to ensure complete polymerization, creating a hard top coat. The thickness of the polymer/cholesteric LC layer was measured using a Fogale Zoomsurf 3D interferometer. The transmission spectra were taken on a Shimadzu UV-3102. Polarizer microscopy images were taken on a Leica microscope equipped with polarizers.

Results and discussion

For the fabrication of single substrate encapsulated reflective films, a mixture consisting of almost equal amounts of a non-polymerizable cholesteric liquid crystalline mixture (nematic MLC-6653 doped with chiral dopant S1011) and polymerizable isotropic monomers (IBMA and BPAMA) was used. The concentration of the S1011 chiral dopant was chosen so the reflection band is in the visible range for viewing by the naked eye, but the position of the reflection notch can easily be shifted to almost any wavelength by adjusting the concentration of the chiral dopant (*vide infra*).[29] IBMA was chosen as it is a non-volatile, low-viscosity polymerizable monomer transparent to visible light after polymerization. The glass transition temperature of poly-(IBMA) is 110 °C, sufficiently high enough to use this polymer as a hard top coating. BPAMA was chosen to crosslink the poly-(IBMA) chains to enhance the rigidity of the polymer coating.

The mixture was spread over the flexible polycarbonate substrate using bar coating as depicted in Fig. 1b. The substrate was used as-is without any alignment layers or chemical treatments. During illumination, a UV light gradient was created throughout the thickness of the film due to absorption of incident UV light by the

absorbing Tinuvin-328,[30] resulting in a higher intensity of the light at the top (closer to lamp) than at the bottom of the coating. This causes faster polymerization of the reactive monomers (IBMA and BPAMA) at the top of the coating than at the bottom, leading to the depletion of reactive molecules at the top, resulting in concentration-driven diffusion of these molecules from the bottom to the top of the coating. The solubility of poly-(IBMA–BPAMA) continuously decreases during polymerization, until finally its phase separates from the rest of the components, resulting in the formation of a polymer encapsulation layer close to the lamp side, leaving the rest of the LC components underneath, as previously reported.[31] In this way, two distinct layers, a cholesteric LC with a striking orange reflective color contained within an encapsulating polymer layer, are formed during this photo-enforced stratification process. The thickness of the polymerized coating was measured to be ∼30 μm using interferometry.

Fig. 2a and b show the transmission spectra of the coating before and after polymerization, respectively, and show that the coating is transparent to visible light before polymerization (see also Fig. 2d(i)). After completing the photo-enforced stratification process, a reflection band centered at 610 nm was observed (Fig. 2b), and the color of the coating changes from transparent to orange upon polymerization (Fig. 2d(ii)). When the same fraction of the chiral dopant was incorporated in the nematic host in a cell construction, the reflection band is almost the same (λ_0 = 570 nm) (Fig. 2c), revealing successful stratification. The minor 40 nm difference in the position of the reflection notch between the encapsulated and cell samples is likely due to the interaction of the LC molecules with the other components in the coating mixture. Fig. 2d(iii) demonstrates that this coating is flexible and can be twisted without damaging its optical properties. The green color visible near the edges upon twisting is due to the angular dependence of the Bragg-like reflector:[16,32] the reflector returns to its initial orange color upon unbending the foil (Fig. 2d(iv)).

The time-dependent appearance of birefringence was monitored to follow the formation of the two layers from the single applied
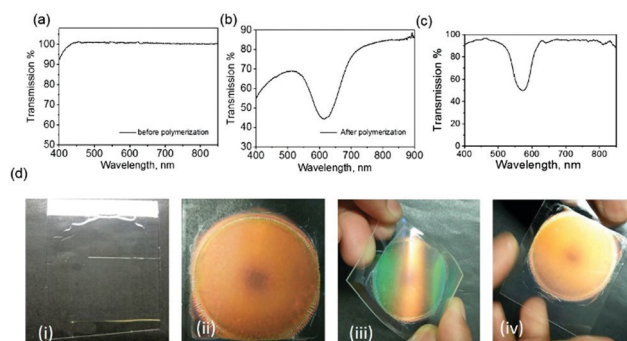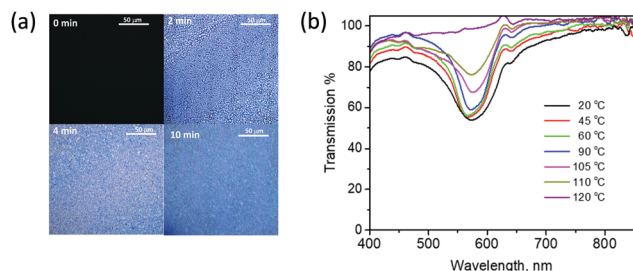

Fig. 2 Transmission spectra of the LC coating on a polycarbonate foil (a) before and (b) after polymerization, and (c) a filled cell containing only LC and 7.9 wt% chiral dopant S1011 composition as in the coating. (d) Photographs of the coating on the polycarbonate foil (i) before polymerization, (ii) after polymerization, with (iii) showing the flexibility of the sample and (iv) after unbending the foil.

Fig. 3 (a) The polarized optical microscopy images of the coating after illuminating with 365 nm light from 0 to 10 minutes. (b) The temperature-dependent transmission spectra of the stratified coating containing S1011 as the chiral dopant on polycarbonate foil.

coating. Fig. 3a shows the optical microscopy images under crossed polarizers. Before polymerization (at t = 0 min), the coating is black under crossed polarizers due to its isotropic nature. After 2 minutes of exposure to UV-light, the coating becomes birefringent and small droplets were observed, likely the result of the phase separation of the LC molecules from the polymer materials. Within 10 minutes of illumination, the droplets coalesce with other droplets and form a continuous layer, forming the stratified LC and polymer layers. No additional changes in the microscopic image were observed upon further UV-light exposure.

Upon heating the coating from 20 °C to 110 °C (see Fig. 3b), some narrowing in the reflection band was observed, probably due to a decrease in the birefringence of the cholesteric LCs.[33] Once the coating was heated to the isotropic state at 120 °C, the reflection band was completely lost and could not be recovered. This could be due to misalignment of the LCs to a focal conic state upon cooling the reflector from the isotropic state.

The single stratification steps so far described create a simple layered structure, but with minimal adherence between the top and bottom layers, limiting the structural integrity of the device. To improve robustness, a preliminary effort was made to attach the top and bottom surfaces, accomplished by way of a two-stage polymerization procedure. The initial illumination of the bar-coated film was through a sputtered metallic mask on glass with 405 nm light at a higher intensity for 3 minutes to minimize horizontal diffusion of the monomers, and directly form wall-like structures through the depth of the film. The mask was removed, and the film exposed to low intensity 365 nm light for 20 minutes, allowing the vertical diffusion of the remaining material to form a solid top layer, followed by a flood exposure at a higher dose to complete polymerization. The procedure may be seen in Fig. 4a. A photograph of the anchored film may be seen in Fig. 4b. The films maintained the capability to be bent and returned to their initial, flat state without obvious damage: see Fig. 4c.

To employ this coating on windows to save energy in the built environment by selectively reflecting excess infrared radiation in response to varying environmental conditions, a temperature responsive cholesteric LC mixture was used (see Experimental section). The temperature responsive chiral dopant (TCD),[34] which has a helical twisting power (HTP) that increases with temperature (resulting in a blue shift in the reflection band), was employed in place of the static S1011 chiral dopant coating for

Fig. 4 (a) The production method of the anchored films. First, exposure of the LC/monomer blend was done with 405 nm light at high intensity through a mask to establish ∼20 μm wide 'walls', followed by removal of the mask and exposure at 365 nm to promote vertical displacement and polymerization of the top layer. (b) Photograph of a microscopy image of the resulting polymerized film. (c) Photograph of the polymerized film on a polycarbonate substrate being bent to an extreme angle to show the adhesion and robustness of the system.
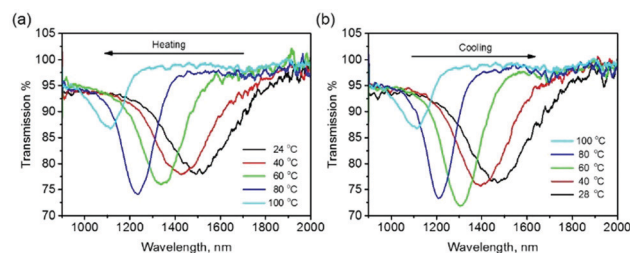
Fig. 5 The transmission spectra of a stratified coating containing a temperature-responsive chiral dopant on the polycarbonate foil upon (a) heating and (b) cooling.

fabricating encapsulated responsive cholesteric LC IR reflectors, the film being produced using the same technique as for the visible reflectors. The amount of chiral dopant was chosen so that the reflection band is centered in the long solar wavelength region (λ_0 = 1500 nm). As shown in Fig. 5a, on heating the coating from 24 °C to 100 °C the reflection band blue-shifted 400 nm. This coating can be subsequently cooled to room temperature to attain the original reflection band (Fig. 5b), demonstrating its reversibility. Again, heating the device beyond the isotropic transition temperature permanently destroyed the reflection of the system. For long-term application, care must be taken to retain the integrity of the polymer seal to avoid leakage/evaporation of the low molecular weight liquid crystal content.

Conclusions

Photo-enforced stratification may be used to fabricate an encapsulated cholesteric LC on a flexible substrate, with a hard polymer layer topping a low molecular weight cholesteric LC reflector. In this way, an iridescent reflector can be created which may be repeatedly bent and returned to its initial state with no obvious damage. A temperature-responsive reflecting

coating which undergoes a blue shift of 400 nm in the infrared region at elevated temperatures could be fabricated using the same technique but changing the chiral dopant. Such responsive coatings could be used for retrofitting existing windows to reflect excess solar IR radiation in response to changing environmental temperature, and energy otherwise spent on heating and cooling could be saved. Higher energy (the shorter wavelength region) solar radiation could be reflected at higher temperatures, whereas this same light could be allowed to enter indoor spaces in lower external temperature conditions so that the indoor temperature could be maintained. One can also imagine applications in textiles or other applications requiring flexibility.

Conflicts of interest

There are no conflicts to declare.

Acknowledgements

References

1 E. P. A. Van Heeswijk, A. J. J. Kragt, N. Grossiord and A. P. H. J. Schenning, *Chem. Commun.*, 2019, **55**, 2880–2891.

2 L. Wang, A. M. Urbas and Q. Li, *Adv. Mater.*, 2018, **1801335**, 1–42.

3 Y. Fang, S. Y. Leo, Y. Ni, J. Wang, B. Wang, L. Yu, Z. Dong, Y. Dai, V. Basile, C. Taylor and P. Jiang, *ACS Appl. Mater. Interfaces*, 2017, **9**, 5457–5467.

4 Y. Liu, J. Lv and L. Lamboni, *Bioinspired Materials Science and Engineering*, John Wiley & Sons, Inc., e-book, 2018, pp. 267–293.

5 H. K. Bisoyi, T. J. Bunning and Q. Li, *Adv. Mater.*, 2018, **30**, 1–35.

6 M. T. Brannum, A. M. Steele, M. C. Venetos, L. S. T. J. Korley, G. E. Wnek and T. J. White, *Adv. Opt. Mater.*, 2019, **7**, 1–7.

7 Y. Wang, Z. G. Zheng, H. K. Bisoyi, K. G. Gutierrez-Cuevas, L. Wang, R. S. Zola and Q. Li, *Mater. Horiz.*, 2016, **3**, 442–446.

8 https://ec.europa.eu/energy/en/topics/energy-efficiency/energy-performance-of-buildings, Accessed May 13, 2019.

9 H. Khan and M. Asif, *Sustainability*, 2017, **9**, 640.

10 L. W. Davis and P. J. Gertler, *Proc. Natl. Acad. Sci. U. S. A.*, 2015, **112**, 5962–5967.

11 M. H. Oh, K. H. Lee and J. H. Yoon, *Energy Build.*, 2012, **55**, 728–737.

12 H. Khandelwal, A. P. H. J. Schenning and M. G. Debije, *Adv. Energy Mater.*, 2017, **7**, 1602209.

13 C. M. Lampert, *Sol. Energy Mater.*, 1981, **6**, 1–41.

14 J. Wang, L. Zhang, L. Yu, Z. Jiao, H. Xie, X. W. Lou and X. Wei Sun, *Nat. Commun.*, 2014, **5**, 4921.

15 L. Zhang, M. Wang, L. Wang, D. Yang, H. Yu and H. Yang, *Liq. Cryst.*, 2016, **43**, 750–757.

16 H. Khandelwal, R. C. G. M. Loonen, J. L. M. Hensen, A. P. H. J. Schenning and M. G. Debije, *J. Mater. Chem. A*, 2014, **2**, 14622–14627.

17 H. Khandelwal, G. H. Timmermans, M. G. Debije and A. P. H. J. Schenning, *Chem. Commun.*, 2016, **52**, 10109–10112.

18 T. D. Nguyen, L. P. Yeo, T. C. Kei, D. Mandler, S. Magdassi and A. I. Y. Tok, *Adv. Opt. Mater.*, 2019, 1801389.

19 Y. Wang, E. L. Runnerstom and D. J. Milliron, *Annu. Rev. Chem. Biomol. Eng.*, 2016, **7**, 1–22.

20 X. Liang, S. Guo, S. Guo, M. Chen, C. Li, Q. Wang, C. Zou, C. Zhang, L. Zhang and H. Yang, *Mater. Horiz.*, 2017, **4**, 878–884.

21 L. Wang, H. K. Bisoyi, Z. Zheng, K. G. Gutierrez-Cuevas, G. Singh, S. Kumar, T. J. Bunning and Q. Li, *Mater. Today*, 2017, **20**, 230–237.

22 D. Manaila-Maximean, C. Rosu, D. Manaila-Maximean, S. Klosowicz, K. Czuprynski, J. Gilli and M. Aleksander, *Mol. Cryst. Liq. Cryst.*, 2010, **417**, 199–205.

23 H. Khandelwal, PhD thesis, Eindhoven University of Technology, 2017.

24 H. Khandelwal, M. G. Debije, T. J. White and A. P. H. J. Schenning, *J. Mater. Chem. A*, 2016, **4**, 6064–6069.

25 M. E. McConney, V. P. Tondiglia, J. M. Hurtubise, L. V. Natarajan, T. J. White and T. J. Bunning, *Adv. Mater.*, 2011, **23**, 1453–1457.

26 L. V. Natarajan, J. M. Wofford, V. P. Tondiglia, R. L. Sutherland, H. Koerner, R. A. Vaia and T. J. Bunning, *J. Appl. Phys.*, 2008, **103**, 093107.

27 E. P. A. Van Heeswijk, J. J. H. Kloos, N. Grossiord and A. P. H. J. Schenning, *J. Mater. Chem. A*, 2019, **7**, 6113–6119.

28 R. Penterman, S. I. Klink, H. de Koning, G. Nisato and D. J. Broer, *Nature*, 2002, **417**, 55–58.

29 D. Mulder, A. P. H. J. Schenning and C. Bastiaansen, *J. Mater. Chem. C*, 2014, **2**, 6695–6705.

30 D. J. Broer, J. Lub and G. N. Mol, *Nature*, 1995, **378**, 467–469.

31 R. Penterman, PhD thesis, Technische Universiteit Eindhoven, The Netherlands, 2005.

32 J. Yan, Y. Chen, D. Xu and S. T. Wu, *J. Appl. Phys.*, 2013, **114**, 113106.

33 J. Li, S. Gauza and S.-T. Wu, *J. Appl. Phys.*, 2004, **96**, 19.

34 H. Yang, K. Mishima, K. Matsuyama, K.-I. I. Hayashi, H. Kikuchi and T. Kajiyama, *Appl. Phys. Lett.*, 2003, **82**, 2407–2409.